List of relevant revisions:

RC1:

Manuscript:

1. Added a brief clarification in Lines 94–95.
2. Revised the manuscript in Lines 268–274.
3. Added related discussion in Lines 480–486.
4. Added a brief description in Lines 324–327.
5. Revised the discussion in Lines 276–279.

Supplement:

6. Added Fig.S1 to the Supplement.
7. Revised the description of Table S1 in Lines 5–7 in the Supplement.
8. Added a data description as Table S3 in the Supplement.

Dataset:

9. Added a link to the ESSD paper.
10. Added a variable 'grid_area' representing grid-cell area and expanded the dataset description accordingly.

RC2:

Manuscript:

1. Added a brief clarification in Lines 94–95.
2. Added the values of fitting grids in Lines 221–224.
3. Added a brief discussion in Lines 462–463.
4. Added discussion in Lines 367–378.
5. Revised clarification in Lines 112–116.
6. Added clarifications in Lines 153–154 and 162.
7. Revised clarification in Lines 212–215.
8. Corrected values in Lines 514–515.
9. Revised the description in Lines 263–265.

Supplement:

10. Added Table S2 and Figure S6 in the Supplement.
11. Added a data description as Table S3 in the Supplement.

Dataset:

12. Added/updated an Excel file (NOx_national_pointsource_2019_2024.xlsx).

The updated dataset (Version 1.1) is available at https://doi.org/10.5281/zenodo.18923337.

Reply to reviewer #1

The authors present NO_x emissions in China derived from TROPOMI column measurements and wind data. The dataset matches the scope of ESSD. The paper is generally well written and should be published after dealing with the following issues:

We sincerely thank the reviewer for the constructive and positive feedback on our paper. We have carefully addressed all the comments and revised the manuscript accordingly. Detailed point-by-point responses are provided below, with our replies shown in blue and all revisions in the manuscript highlighted in italics.

Data:

1. Please specify the processor version for the used TROPOMI data. Recent processor updates have made some modifications that results in overall higher tropospheric VCDs, which would affect the discussion of the observed low bias in emissions.

Response: In this study, we use the operational offline TROPOMI NO_2 TVCD product (S5P_L2__NO2___HiR2) from NASA GES DISC. As discussed in Line 494–496, this work primarily aims to propose a practical and insightful perspective for addressing nonlinear NO_x chemistry in emissions estimation, rather than focusing on improvements in retrieval data quality (e.g., air mass factor corrections in satellite NO_2 retrievals). The standard operational NO_2 product is selected, and additional corrections are expected to improve estimation accuracy. We added a brief clarification **in Lines 94–95**: *The operational offline TROPOMI NO_2 TVCD product (S5P_L2__NO2___HiR2) (Van Geffen et al., 2024) from NASA GES DISC (https://daac.gsfc.nasa.gov/datasets/) for 2019–2024 is used in this study.*

Methods:

2. The authors refer to previous work, in particular Ayazpour et al. It is not clear to me how far the current dataset is derived from the method described in Ayazpour, or if modifications/extensions have been made. Please explicitly specify what is new/different in this study as compared to Ayazpour.

Response: The current study builds on the DDA framework by Sun (2022) and its modification by Ayazpour et al. (2025), introducing two main improvements: the application of GEOS-CF chemical data in the modified DDA to better capture strong NO_x gradients near point sources, and the piecewise fitting approach to obtain nonlinear NO_x lifetimes, while the latter represents the main improvement in this study. Figure 3 compares the three DDA-based approaches, illustrating the differences between the original framework, the modified version, and the current study.

We revised the manuscript **in Lines 268–274** as follows: *To illustrate the developments in this study, Figure 3 compares three DDA-based results before and after applying the NO_x/NO_2 ratio correction and improved fitting scheme: (1) a constant NO_x/NO_2 ratio of 1.32 and monthly single-lifetime fitting (fixed_f and single_τ), corresponding to the original DDA framework by Sun (2022); (2) the variable NO_x/NO_2 ratio and monthly single-lifetime fitting (variable_f and single_τ), based on the modification by Ayazpour et al. (2025) and marking the first application of GEOS-CF chemical data in satellite-based emission estimation; (3) a combination of the variable NO_x/NO_2 ratio and piecewise fitting with nonlinear NO_x lifetimes for each month (variable_f and nonlinear_τ), while the latter represents the major improvement in this study.*

3. The lifetime and inverse scale height are fitted based on Eq. (3) for different levels of NO_2 VCDs. However, the basic assumption for this is that emissions are negligible. While this is a good

approximation over remote regions (most parts of WN and WS), I wonder how far this assumption can be made over EN for high NO_2 VCDs. Please extend the discussion accordingly.

Response: As noted by the reviewer , fitting is performed over grid cells with negligible local emissions to isolate the effects of transport, topography, and chemical loss. These locations do not necessarily have low NO_2 columns, as elevated NO_2 TVCDs may result from transport from upwind sources. The fitted scale heights and chemical lifetimes thus reflect effective subregional characteristics rather than strictly local source effects. Piecewise fitting across NO_2 TVCD bins allows pixels with higher NO_2 columns to contribute to the lifetime regression, capturing nonlinear NO_x chemistry; Fig. 1 shows an example of lifetime fitting using high-percentile NO_2 TVCD grids in each subregion. Nevertheless, assuming spatially homogeneous scale heights may lead to overestimation in heavily polluted areas, and lifetimes may still exhibit spatial heterogeneity within each subregion.

We added related discussion **in Lines 480–486**: *The fitted scale heights and chemical lifetimes represent effective subregional parameters derived from grid cells with negligible local emissions, which may lead to overestimation of scale heights in heavily polluted areas and do not fully reflect the sensitivity of NO_x lifetimes to environmental conditions, although the regional averages still capture nonlinear NO_x chemistry. As these are fitting parameters, their physical interpretation should be treated cautiously to avoid over-interpretation (Lonsdale and Sun, 2023). Future observations with higher spatial resolution could improve the representation of scale height and chemical lifetime across heterogeneous regions.*

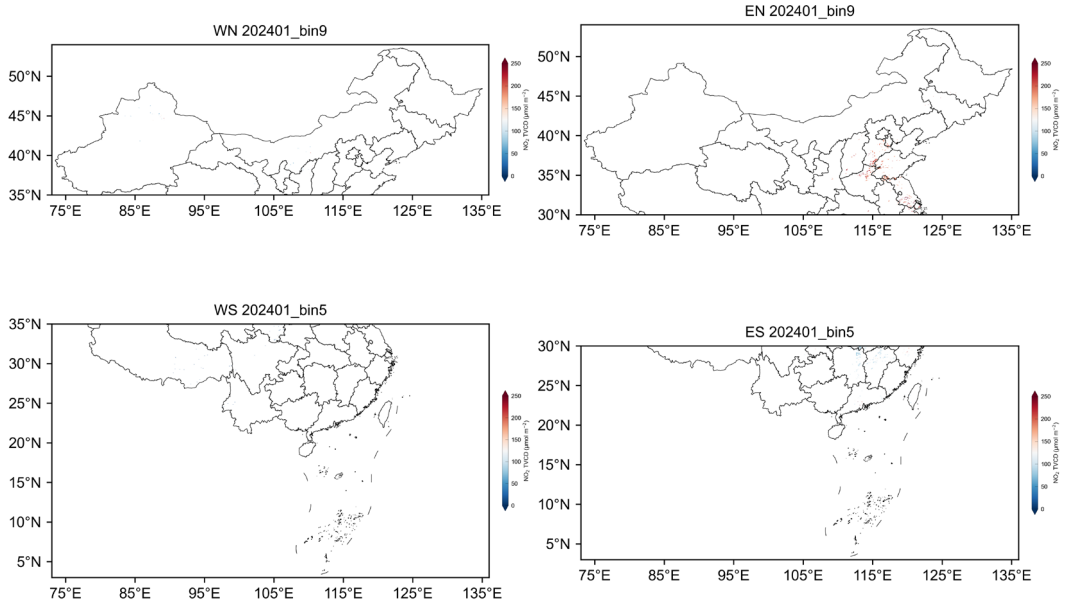

Figure 1. Example of lifetime fitting using high-percentile NO_2 TVCD grids in each subregion, with the number of grids ranging from 48 to 790.

Results:

4. Fitted lifetimes are presented in Fig. 4 and discussed in the text. Please provide and discuss the results for scale height as well. I would expect that scale height increases with distance from source regions, i.e., the assumption of constant X needs to be discussed. I would also expect that X might change seasonally due to different lifetimes.

Response: We added **Fig.S1 to the Supplement** to compare the three DDA-based scale height ($1/X$) for four subregions. The results show clear seasonal variability as well as regional differences. In general,

X is higher in the cleaner and more remote regions (WN and WS) than in the more polluted regions (EN and ES). In the DDA framework, X represents the inverse scale height defined as $X = C|_{z_0}/\Omega$, where Ω is the NO_2 TVCD and $C|_{z_0}$ is NO_2 surface concentration (Sun, 2022). X links the surface concentration to the vertical column density. Since X mainly reflects the effective vertical mixing depth, its variability is primarily controlled by boundary layer mixing rather than chemical lifetime. Consequently, seasonal changes in X are expected and do not necessarily follow the seasonal variation of NO_x lifetime.

We added a brief description **in Lines 324–327**: *In addition, the scale height ($1/X$) fitting results for each subregion are presented in Fig. S1. Scale height shows clear seasonal and regional variability, generally higher in the cleaner and more remote regions (WN and WS) than in the more polluted regions (EN and ES). Its variability is primarily controlled by boundary layer mixing, as X links surface concentration to column density, reflecting the effective vertical mixing depth (Lonsdale and Sun, 2023; Sun, 2022).*

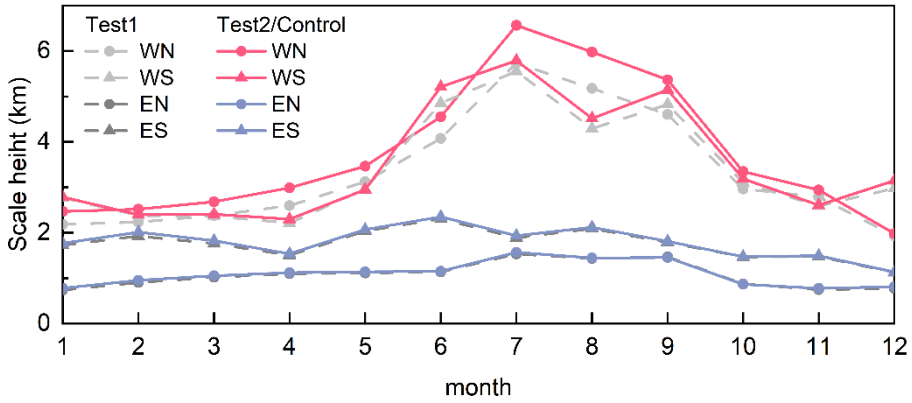

Figure S1. Comparison of monthly scale height (1/X) among three DDA-based setups for each subregion. Test1, Test2, and Control setups are the same as defined in Table S1. The X values are identical for Test2 and the Control setup because both share the same components in the modified DDA framework with variable NO_x/NO_2 ratio.

5. Table S1: Lifetimes for the test setups are far longer that for control, and also far longer than those reported in several recent studies that estimated NO_x lifetimes of the order of 5 hours from (TROP)OMI NO_2 patterns downwind strong sources. What is the reason for the large lifetimes in the test setups? At the same time, fit performance seems to be often better in the test setups than in the control setup. Please comment.

Response: As noted by the reviewer, NO_x lifetimes derived in test1 and test2 are substantially longer than those reported in previous studies. This mainly arises from the fitting strategy. In test1 and test2, a single τ is fitted over relatively clean regions, which tends to overestimate the chemical lifetime. When this single lifetime is applied across the entire study domain, it weakens the effective chemical loss term and introduces an imbalance among local emissions, horizontal transport, and chemical loss. As a result, a considerable number of negative emission grids are reduced, the inferred NO_x flux is underestimated, and the applicability of the lightweight method is limited when extending from point-source to regional emission estimation.

The control setup accounts for nonlinear behavior through piecewise lifetime fitting, yielding shorter and more physically consistent lifetimes. We revised the discussion **in Lines 276–279** to clarify this point as follows: *The nonlinear lifetime fitting more effectively accounts for the balance among local emissions,*

horizontal transport, and chemical loss, reducing negative emission grids and increasing regional emission estimates. Consequently, the improved fitting scheme minimizes artifacts in mountainous and remote regions compared to earlier results (Ayazpour et al., 2025; Beirle et al., 2023; Lonsdale and Sun, 2023; Sun, 2022).

Table S1 compares the lifetime fitting parameters among the three DDA-based setups. In test1 and test2, fitting is applied once over each subregion, yielding a single τ per month. In the control setup, τ is fitted across NO_2 TVCD percentile-based piecewise bins for each month and subsequently averaged for each subregion (Lines 212–226); R^2 and RMSE are the associated fitting statistics referring to the τ fitting. Thus, in Table S1, R^2, RMSE and τ denote the corresponding monthly means across the piecewise bins. For all piecewise bins in EN, R^2 ranges 0.02–0.96, with monthly means in Table S2 of 0.29–0.68; RMSE ranges 0.07–2.3 µmol m^{-2} s^{-1}, with monthly means of 0.25–0.83 µmol m^{-2} s^{-1}; and τ ranges 2.35–17.74 h, with monthly means of 5.10–8.38 h. Compared with test1 and test2, the fit performance of the control setup is more variable across bins, with some bins performing better and others worse. To facilitate comparison, Table S1 lists the monthly means. Overall, the control setup shows more variable performance across bins and higher RMSE than test1/test2, mainly because bins with higher NO_2 TVCDs disproportionately increase the monthly RMSE.

We revised the description of Table S1 **in Lines 5–7 of the Supplement** to clarify this issue: *All values are monthly means: for test1 and test2, the monthly mean is calculated from a single fit over the subregion; for the control setup, the monthly mean is calculated by averaging the piecewise bin results for the subregion. The bottom row shows the mean over the entire study period.*

Dataset:

6. Data is provided on zenodo in form of annual nc files. The data is easily accessible and readable. The following items should be clarified/improved:

Please provide some further information how this data was generated or just add a link to the ESSD paper to the attributes.

Response: We added a link to the ESSD paper on the download page as suggested by the reviewer.

7.Please specify the molecular mass the given emissions are referring to (NO_2?)

Response: As noted by the reviewer, we clarify this issue **in Lines 178–179** as follows and emphasize it in the dataset description: *All bracketed terms are averaged at a monthly scale before X and τ are fitted (see in Sect. 3.2) to derive emissions ⟨EE⟩ in mol m^{-2} s^{-1}, and the conversion to mass assumes NO_x as NO_2.*

8. The unit "tons" is misleading, as this is used differently in e.g., Europe (metric tons) and the US ("short ton"). Please switch to SI units, e.g., 1e3 kg. The given emissions are just given in tons.

Response: The manuscript uses t and kt, referring to metric tonnes (1 t = 1 tonne =10^3 kg; 1 kt = 10^3 tonnes). The dataset annotation uses tonnes, which also denotes metric tonnes. We added a data description as **Table S3 in the Supplement**.

9. From the context, I conclude that these values are referring to "per year" (as there are annual files) and "per pixel". This should be clarified. Due to the link to "pixel", the results depend on the chosen grid, and can NOT be simply interpolated for comparisons to other data. I would thus recommend to switch to emission rate densities (mass per time per area), which then could be easily interpolated and integrated

to any other grid. Then also the unit would be self-explaining. In any case, I recommend to add an additional field "area" (lat coordinate only) which would allow for easy conversion between densities and integrated values by the user.

Response: As noted by the reviewer, the dataset provides gridded anthropogenic NO_x emissions per year per grid (at 0.05° × 0.05° resolution), which represent emission totals rather than emission rate densities. To facilitate potential conversion to emission rate densities (mass per time per area), we added a variable 'grid_area' representing grid-cell area and expanded the dataset description accordingly.

The updated dataset (Version 1.1) is available at https://doi.org/10.5281/zenodo.18923337 (Chen et al., 2026).

We sincerely appreciate the reviewer's thoughtful comments and suggestions, which helped improve both the manuscript and the dataset.

References

Ayazpour, Z., Sun, K., Zhang, R., and Shen, H.: Evaluation of the Directional Derivative Approach for Timely and Accurate Satellite-Based Emission Estimation Using Chemical Transport Model Simulation of Nitrogen Oxides, Journal of Geophysical Research: Atmospheres, 130, e2024JD042817, https://doi.org/10.1029/2024JD042817, 2025.

Beirle, S., Borger, C., Jost, A., and Wagner, T.: Improved catalog of NO_x point source emissions (version 2), Earth Syst. Sci. Data, 15, 3051–3073, https://doi.org/10.5194/essd-15-3051-2023, 2023.

Chen, L., Cai, Z., Sun, K., Liu, Y., Yang, D., Li, M., and Zhu, L.: Regional and point source nitrogen oxides emissions in China from TROPOMI, https://doi.org/10.5281/zenodo.18923337, 2026.

Lonsdale, C. R. and Sun, K.: Nitrogen oxides emissions from selected cities in North America, Europe, and East Asia observed by the TROPOspheric Monitoring Instrument (TROPOMI) before and after the COVID-19 pandemic, Atmos. Chem. Phys., 23, 8727–8748, https://doi.org/10.5194/acp-23-8727-2023, 2023.

Sun, K.: Derivation of Emissions From Satellite-Observed Column Amounts and Its Application to TROPOMI NO_2 and CO Observations, Geophysical Research Letters, 49, e2022GL101102, https://doi.org/10.1029/2022GL101102, 2022.

Reply to reviewer #2

This manuscript presents a comprehensive dataset of satellite-derived NO_x emissions over China for 2019–2024, based on an enhanced Directional Derivative Approach (DDA). The resulting dataset is spatially resolved, covers both regional and point-source emissions, and is validated against multiple bottom-up inventories and independent top-down products. The work is clearly within the scope of ESSD. Overall, the manuscript is well written and supported by extensive analysis. However, several methodological assumptions require further clarification. I therefore recommend publication after these revisions. The paper is generally well written and should be published after dealing with the following issues:

We are grateful to the reviewer for the positive assessment of our manuscript and for the constructive comments on the methodological assumptions. We have carefully addressed all comments and revised the manuscript accordingly. Detailed point-by-point responses are provided below, with our replies shown in blue and all revisions highlighted in italics.

Method and results:

1. Please explicitly state the TROPOMI NO_2 product version used in the proposed method.

Response: The operational offline TROPOMI NO_2 TVCD product (S5P_L2__NO2___HiR2) from NASA GES DISC is used in this study. As discussed in Line 494–496, this work primarily aims to propose a practical and insightful perspective for addressing nonlinear NO_x chemistry in emissions estimation, rather than focusing on improvements in retrieval data quality (e.g., air mass factor corrections in satellite NO_2 retrievals). The standard operational NO_2 product is selected, and additional corrections are expected to improve estimation accuracy. We added a brief clarification **in Lines 94–95**: *The operational offline TROPOMI NO_2 TVCD product (S5P_L2__NO2___HiR2) (Van Geffen et al., 2024) from NASA GES DISC (https://daac.gsfc.nasa.gov/datasets/) for 2019–2024 is used in this study.*

2. The piecewise fitting of NO_x lifetime as a function of NO_2 TVCD percentile and subregion (Sect. 3.2) is a key innovation of this work. Please provide additional information on: The minimum number of grid cells per bin used for fitting and Whether a smoother functional form (rather than piecewise bins) was tested. A clearer discussion would strengthen the methodological transparency.

Response: NO_x lifetime is fitted for each individual month and subsequently averaged for the same month within each subregion over the study period. After data retrieval and fitting threshold filtering, a total of 1393 month-bins are successfully fitted across the four subregions. The number of grid cells per bin ranges from 3 to 9388 (10^{th} percentile: 17; median: 91; mean: 199), indicating that most bins contain sufficient data for robust lifetime fitting, while bins with very small sample sizes are rare and have negligible influence on the overall regression. The mean lifetime for each month-bin is calculated by averaging the successfully fitted bins across all years. The number of grid cells contributing to each month-bin mean ranges from 8 to 38,610 (10^{th} percentile: 67; median: 382; mean: 789). We added the values **in Lines 221–224**: *A total of 1393 month-bins are successfully fitted across the four subregions. The number of grid cells per bin ranges from 3 to 9388 (10^{th} percentile: 17; median: 91; mean: 199), indicating that most bins contain sufficient data for robust lifetime fitting, while bins with very small sample sizes are rare and have negligible influence on the overall regression.*

NO_x lifetime first increases at very low NO_x concentrations, then decreases at moderate levels, and can rise again at very high NO_x due to the "NO_x-suppressed" regime (Lange et al., 2022; Pusede et al., 2015). This nonlinear behavior is difficult to describe with a single smooth function. The piecewise fitting scheme combines multiple linear fits across NO_2 TVCD bins, using the NO_x concentrations that affect lifetime as references while accounting for regional background conditions, providing a simple and robust approach to represent nonlinear NO_x chemistry in the DDA framework. We added a brief discussion **in Lines 462–463**: *This scheme combines multiple linear fits based on NO_2 TVCD levels, providing a simple and robust way to represent nonlinear NO_x chemistry in the DDA framework.*

3. Please quantify how national anthropogenic totals change under alternative assumptions (e.g., different NTL thresholds or without subtracting soil emissions). This will help users better interpret the dataset.

Response: We added **Table S2 and Figure S6 in the Supplement** to support the choice of the NTL threshold. The results indicate that without applying the NTL constraint, anthropogenic NO_x emissions

would be underestimated by 5.4–15.1%. In contrast, the differences among results obtained with different NTL thresholds are relatively small (−4.9% to 3.6%). Furthermore, if soil and biomass burning NO_x emissions from grids not classified as natural sources are not subtracted using the inventory, anthropogenic NO_x emissions would be overestimated.

The corresponding discussion has been added **in Lines 367–378** as follows: *Table S2 shows NO_x emissions from sensitivity tests of the anthropogenic NO_x filter threshold, and Figure S6 presents the probability density function (PDF) of nighttime light (NTL) to support the selection of the NTL threshold. The results indicate that without applying the NTL constraint, anthropogenic NO_x emissions would be underestimated. The differences among results obtained with different NTL thresholds are relatively small (−4.9% to 3.6%). Under the selected threshold of 0.01 nW cm^{-2} sr^{-1}, more than 90% of NTL grids are identified as anthropogenic sources, and this threshold also helps minimize the resampling effect from 500 m to 0.05° in dark regions. Overall, the small differences among different thresholds and the good agreement with other datasets demonstrate the robustness of the anthropogenic NO_x source filtering approach used in this study.*

Table S2. NO_x emissions from sensitivity tests of the anthropogenic NO_x filter threshold.

This work (NTL_0.01): Grid cells with either the highest averaged NO_2 TVCDs in summer or the lowest values in winter comparing to other seasons, and with NTL < 0.01 nW cm^{-2} sr^{-1}, are subtracted as natural NO_x (NO_x_nat), and for the remaining grid cells, soil and biomass burning emissions (from CAMS data) are further subtracted to obtain anthropogenic NO_x (NO_x_anthro);

NTL_none: Same as this work, but without applying the NTL filter;

NTL_0.00: Same as this work, but with NTL = 0.00 nW cm^{-2} sr^{-1};

NTL_0.05: Same as this work, but with NTL < 0.05 nW cm^{-2} sr^{-1};

CAMS_none: Same as this work, but soil and biomass burning emissions from CAMS data are not subtracted;

NTL_anthro: Fraction of NTL grids that are also classified as anthropogenic NO_x grids.

Year	Variable	Test				
		This work (NTL_0.01)	NTL_none	NTL_0.00	NTL_0.05	CAMS_none
2019	NO_x_anthro (Tg)	20.2	18.9	20.7	19.7	21.3
	NO_x_nat (Tg)	9.6	11.0	9.2	10.1	9.6
	NTL_anthro (%)	93.0	77.4	100.0	85.5	93.0
2020	NO_x_anthro (Tg)	18.5	17.3	18.9	18.1	19.6
	NO_x_nat (Tg)	10.3	11.5	9.9	10.7	10.3
	NTL_anthro (%)	93.5	78.1	100.0	86.7	93.5
2021	NO_x_anthro (Tg)	19.4	18.3	19.7	19.0	20.5
	NO_x_nat (Tg)	9.3	10.4	9.0	9.7	9.3
	NTL_anthro (%)	94.1	81.6	100.0	88.1	94.1
2022	NO_x_nat (Tg)	18.9	17.2	19.4	18.3	20.0
	NO_x_nat (Tg)	9.3	11.0	8.8	9.9	9.3
	NTL_anthro (%)	93.2	74.7	100.0	85.0	93.2
2023	NO_x_anthro (Tg)	20.7	17.7	21.3	19.8	21.8
	NO_x_nat (Tg)	8.1	11.0	7.4	9.0	8.1
	NTL_anthro (%)	92.6	66.9	100.0	83.0	92.6
2024	NO_x_anthro (Tg)	18.8	16.0	19.5	17.9	19.9
	NO_x_nat (Tg)	8.5	11.4	7.9	9.5	8.5

NTL_anthro (%)	*92.0*	*67.4*	*100.0*	*82.0*	*92.0*

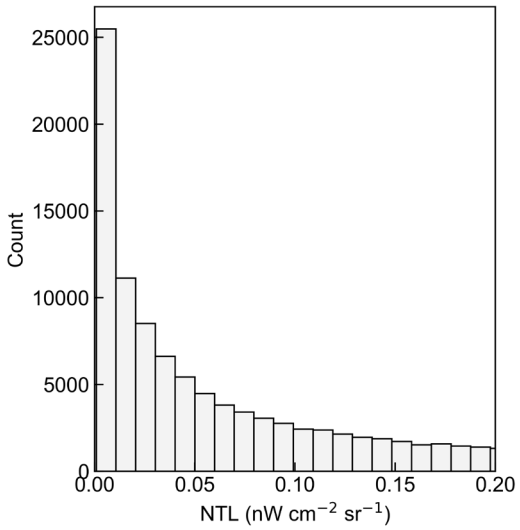

Figure S6. Probability density function (PDF) of SNPP/VIIRS Nighttime Light (NTL) in China in 2023.

4. Line 22–24: "first application of a lightweight, satellite-driven method" — please clarify "first" relative to previous DDA/FDA-based studies (e.g., Beirle et al., Ayazpour et al.).

Response: Two key challenges remain for NO_x emission estimation using the FDA and DDA, including the NO_x/NO_2 ratio and the nonlinear NO_x lifetime. Previous studies have accounted for spatial variability of NO_x/NO_2 ratios using auxiliary data (Beirle et al., 2021, 2023; Ayazpour et al., 2025; Cifuentes et al., 2025; Meier et al., 2024) and explored factors (Beirle et al., 2023; Lange et al., 2022; Krol et al., 2024; Meier et al., 2024) to represent lifetime variability. However, capturing nonlinear NO_x chemistry (Laughner and Cohen, 2019) remains difficult (in Lines 70–84). As a result, estimated emissions often contain a considerable number of negative grids due to imbalances among local emissions, horizontal transport, and chemical loss, limiting the applicability of lightweight methods when extending from point sources (Beirle et al., 2019, 2021, 2023; Sun, 2022) or individual cities (Cifuentes et al., 2025; Lonsdale and Sun, 2023) to regional emission estimation (in Lines 276–279 and 506–513).

In this work, by incorporating a spatially variable NO_x/NO_2 ratio and implementing a data-driven, piecewise fitting strategy, we extend the lightweight satellite-based DDA framework to estimate both point-source and regional NO_x emissions across China. In this context, "first" refers to *the application of a lightweight, satellite-driven NO_x emissions estimator in such a large and topographically complex region* (in Lines 19–21 and 511–513).

5. Line 114–118: Justify the use of near-surface NO_x/NO_2 ratios for column-based inversion more explicitly.

Response: We revised the manuscript for clarity **in Lines 112–116**: *The NO_x/NO_2 ratios are highest near emission sources because freshly emitted NO rapidly consumes local ozone and is subsequently oxidized to NO_2 as the plume mixes with background air (Meier et al., 2024). Following Beirle et al. (2021, 2023), NO_2 columns are converted to NO_x using the near-surface photostationary state, with the NO_x/NO_2 ratio from the near-surface model layer with a 1-hour temporal resolution (chm_tavg_1hr_g1440x721_v1) used in this study to better represent near-source conditions and*

the resulting NO_x gradients (Ayazpour et al., 2025; Sun, 2022).

6. Eq. (1)–(2): Please define all vector operators and clarify notation for gradients (horizontal or terrain-following).

Response: In Eqs. (1)–(2), ∇ denotes the two-dimensional horizontal vector differential operator in Cartesian coordinates, i.e., $\nabla = (\partial/\partial x, \partial/\partial y)$, No terrain-following coordinate system is used in this formulation. The operator $\langle\rangle$ denotes spatiotemporal averaging. These clarifications have been added to the revised manuscript **in Lines 153–154 and 162**.

7. Line ~223: Clarify whether bins are constructed independently for each month or based on climatological distributions.

Response: We revised the manuscript for clarity **in Lines 212–215**: *Given the small interannual variability and limited impact on reactive species emission estimation (Ayazpour et al., 2025), β_1 is fitted using the same climatological months, whereas β_2 is fitted for each individual month using NO_2 TVCD percentile bins constructed independently for that month and subsequently averaged over the same months for each subregion during 2019–2024.*

8. Line ~495–500: Lifetime ranges reported here differ slightly from Sect. 4.2; please ensure consistency.

Response: We thank the reviewer for pointing this out. We have corrected the discrepancy, and the lifetime ranges are now consistent with those reported in Sect. 4.2 (**in Lines 514–515**).

9. Please clarify whether σ_0 (Eq. 7) includes satellite retrieval noise or only directional variability in DDF.

Response: σ_0 in Fig. 2 is estimated from the standard deviation of the difference between $DDf_{\vec{x}/\vec{y}}$ and $DDf_{\vec{r}/\vec{s}}$, based on 0.05° grids by resampling satellite orbit data. As such, σ_0 inherently includes both the satellite retrieval noise and the random error associated with the DDF estimator (directional variability). We revised the description **in Lines 263–265** as follows: *Therefore, the random error of DDf is employed to characterize the uncertainties in DDA emission estimation, encompassing both satellite retrieval noise and the random error arising from the DDf estimator.*

Dataset:

10. The public availability of the data via Zenodo is strongly appreciated and fully aligns with the mission of Earth System Science Data. Please expand the data description (Sect. 6 or Supplement) to include: A table listing all variables, units, dimensions, and fill values. Explicit statement of whether emissions are reported as NO_2-equivalent mass or NO_x mass.

Response: We added a data description as **Table S3 in the Supplement**.

Table S3. Description of variables in the dataset.

Name	*Description*	*Dimensions*	*Units*	*Fill_value*
lat	*Latitude*	*lat*	*degrees_north*	*NaN*
lon	*Longitude*	*lon*	*degrees_east*	*NaN*
grid_area	*Grid-cell area*	*lat × lon*	*m^2*	*NaN*
NO_x_emission	*Annual anthropogenic NO_x emissions per grid*	*lat × lon*	*tonnes (1 tonne =10^3 kg)*	*NaN*

As noted by the reviewer, we clarify this issue **in Lines 178–179** as follows: *All bracketed terms are averaged at a monthly scale before X and τ are fitted (see in Sect. 3.2) to derive emissions ⟨EE⟩ in mol* m^{-2} s^{-1}*, and the conversion to mass assumes* NO_x *as* NO_2*.*

11. Please clarify whether grid-level or regional uncertainty fields are included in the data files. If not, whether uncertainty estimates are provided at aggregated scales only (e.g., national/provincial).
Response: Grid-level uncertainties are not included in the NetCDF data files, because the regional uncertainties are calculated by aggregating grid-level precision according to Eq. (3). Instead, aggregated uncertainty estimates at national and point-source scales and are added in a separate Excel file (**NOx_national_pointsource_2019_2024.xlsx**).

12. The manuscript notes that the improved fitting scheme reduces negative emission artifacts, but it is unclear how such values are handled in the final dataset. Whether negative grid-cell emissions are retained, masked, or truncated in the released data.
Response: All negative grid-cell emissions are retained in the dataset without masking or truncation to preserve the original inversion results.

13. Please clarify whether future updates (e.g., extension beyond 2024 or revised inputs) are planned.
Response: We plan to extend the dataset beyond 2024 and release updated versions as needed, which will be shared through the same platform.
The updated dataset (Version 1.1) is available at https://doi.org/10.5281/zenodo.18923337 (Chen et al., 2026).

We sincerely thank the reviewer again for the helpful comments that improved both the manuscript and the dataset, as well as for the interest and encouragement regarding the continued development of this method.

References

Ayazpour, Z., Sun, K., Zhang, R., and Shen, H.: Evaluation of the Directional Derivative Approach for Timely and Accurate Satellite-Based Emission Estimation Using Chemical Transport Model Simulation of Nitrogen Oxides, Journal of Geophysical Research: Atmospheres, 130, e2024JD042817, https://doi.org/10.1029/2024JD042817, 2025.

Beirle, S., Borger, C., Dörner, S., Li, A., Hu, Z., Liu, F., Wang, Y., and Wagner, T.: Pinpointing nitrogen oxide emissions from space, Sci. Adv., 5, eaax9800, https://doi.org/10.1126/sciadv.aax9800, 2019.

Beirle, S., Borger, C., Dörner, S., Eskes, H., Kumar, V., De Laat, A., and Wagner, T.: Catalog of NO_x emissions from point sources as derived from the divergence of the NO_2 flux for TROPOMI, Earth Syst. Sci. Data, 13, 2995–3012, https://doi.org/10.5194/essd-13-2995-2021, 2021.

Beirle, S., Borger, C., Jost, A., and Wagner, T.: Improved catalog of NO_x point source emissions (version 2), Earth Syst. Sci. Data, 15, 3051–3073, https://doi.org/10.5194/essd-15-3051-2023, 2023.

Chen, L., Cai, Z., Sun, K., Liu, Y., Yang, D., Li, M., and Zhu, L.: Regional and point source nitrogen oxides emissions in China from TROPOMI, https://doi.org/10.5281/zenodo.18923337, 2026.

Cifuentes, F., Eskes, H., Dammers, E., Bryan, C., and Boersma, F.: Accurate space-based NO_x emission estimates with the flux divergence approach require fine-scale model information on local oxidation chemistry and profile shapes, Geoscientific Model Development, 18, 621–649, https://doi.org/10.5194/gmd-18-621-2025, 2025.

Lange, K., Richter, A., and Burrows, J. P.: Variability of nitrogen oxide emission fluxes and lifetimes estimated from

Sentinel-5P TROPOMI observations, Atmospheric Chemistry and Physics, 22, 2745–2767, https://doi.org/10.5194/acp-22-2745-2022, 2022.

Laughner, J. L. and Cohen, R. C.: Direct observation of changing NO_x lifetime in North American cities, Science, 366, 723–727, https://doi.org/10.1126/science.aax6832, 2019.

Lonsdale, C. R. and Sun, K.: Nitrogen oxides emissions from selected cities in North America, Europe, and East Asia observed by the TROPOspheric Monitoring Instrument (TROPOMI) before and after the COVID-19 pandemic, Atmos. Chem. Phys., 23, 8727–8748, https://doi.org/10.5194/acp-23-8727-2023, 2023.

Meier, S., Koene, E. F. M., Krol, M., Brunner, D., Damm, A., and Kuhlmann, G.: A lightweight NO_2-to-NO_x conversion model for quantifying NO_x emissions of point sources from NO_2 satellite observations, Atmospheric Chemistry and Physics, 24, 7667–7686, https://doi.org/10.5194/acp-24-7667-2024, 2024.

Pusede, S. E., Steiner, A. L., and Cohen, R. C.: Temperature and Recent Trends in the Chemistry of Continental Surface Ozone, Chem. Rev., 115, 3898–3918, https://doi.org/10.1021/cr5006815, 2015.

Sun, K.: Derivation of Emissions From Satellite-Observed Column Amounts and Its Application to TROPOMI NO_2 and CO Observations, Geophysical Research Letters, 49, e2022GL101102, https://doi.org/10.1029/2022GL101102, 2022.